Scaffold Public Documents – **SPD26**

**Innovative strategies, methods and tools for occupational risks management of manufactured nanomaterials (MNMs) in the construction industry**

# HIGH SENSITIVITY DEVICE FOR TRAPPING AEROSOLIZED NANOPARTICLES AND PURIFYING AIR

Scaffold Public Documents - Ref.: Scaffold SPD26

Delphine Boutry, Jean-François Damlencourt (CEA)

19/09/2014

The Scaffold research has received funding from the European Community's Seventh Framework Programme (FP7/20072013) under grant agreement number 280535.

# INDEX

# 1. EXECUTIVE SUMMARY

This report concerns the design and the development of a new device that captures the airborne nanoparticles (NPs) and removes them from the atmosphere. Protection of the human lung from ultrafine particles is difficult with current technologies. High-Efficiency PArticulate air (HEPA) filters remove airborne particles with 99.97% efficiency of 0.3µm, the most penetrating particle size. Smaller and larger particles are filtered at even greater efficiency. But HEPA filters are expensive. ElectroStatic Precipitation (ESP) has been used as inexpensive approach to remove large particles from airflows, but it has a collection efficiency minimum in the submicrometer size range. The overall mass based efficiency of ESPs is of the order of 99%. However, the collection efficiency curve is U-shaped and there is a penetration window in the submicrometer size range where the efficiencies are as low as 70-80%. This is due to the balance between two opposing effects, decreasing charge with decreasing particle size and increasing drag with increasing particle size. Moreover, experimental observations have shown that collection efficiency decreases with decreasing diameter below 60nm [1]. The low capture efficiencies have been attributed to partial charging of these particles. In this case, unipolar corona charging has been found to be inadequate to charge the ultrafine particles efficiently. The solution found was to incorporate soft X-ray irradiation as an *in situ* component of the ESP process to improve capture efficiency of ultrafine particles (sizes of virus, bacteria and small molecules, see Figure 1) and to neutralize bacteria and viruses by irradiating and photoionizating them.

In our study, we investigated the capture efficiency as a function of the applied voltage, the action of the photoionizer, the particles diameter and the chemical nature of the particles. Concerning the applied voltage, we observed and calculated the Inception Corona Voltage (ICV). We observed that finally we do not need Corona voltage to catch efficiently ultrafine particles with sizes ≤100nm and that very low applied voltage was sufficient, even to collect ultrafine particles (25nm). Moreover, we demonstrated that the addition of a soft X-ray irradiation in an ESP resulted in a general increase of the capture efficiency of particles having sizes between 50nm to 100nm. But according to the size of the NPs, we observed that the efficiency of the photoionizer differed and the effect of the soft X-ray irradiation was more important for bigger sizes. Concerning the chemical nature, $TiO_2$ and nanoclays NPs seemed to be the more efficiently collected.

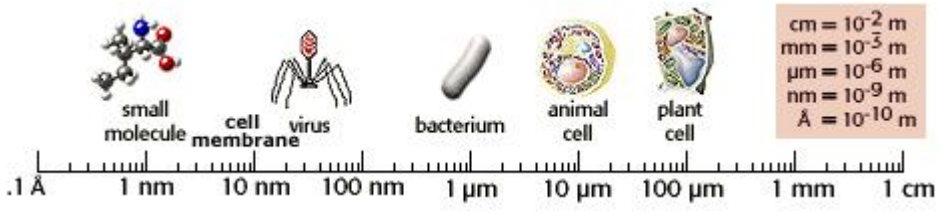


*Figure 1: Relative sizes of cells and their components.*

## 2. OBJECTIVE

The objective of this study was at first to design and to manufacture a soft X-Ray electrostatic precipitation. Different versions have been tested and the main problem was the emission of X-Rays outside the device. Therefore, different type of materials were studied in order to have an emission < 1µSv/h, the limit threshold for humans. Secondly, we tested the capture efficiency using the nanoparticles provided by the industrial partners.
The NPs investigated were:

1) Nano $SiO_2$ given by TECNAN
2) Nano $TiO_2$ given by TECNAN
3) Nanocellulose given by ACCIONA
4) Nanoclay given by Netcomposites

## 3. RESULTS and DISCUSSION

1) The soft X-Ray Electrostatic Precipitation:

The ElectroStatic Precipitation (ESP) electrically charges airborne particles and in presence of an electric field, all the particles are directed and deposited on a metallic collection plate. Generally, particles are charged by the corona generated by a high DC voltage applied across the electrodes. But unipolar corona charging has been found to be inadequate to charge the ultrafine particles efficiently. That's why a soft X-Ray radiation was added because it enhanced photoionization and improved charging of ultrafine particles in a corona. Figure 2 shows the schematic diagram explaining the diffusion, direct particle charging and photoemission processes inside the ESP in the presence of corona and X-ray radiation. Particles can acquire charge either by direct photoionization or by charge diffusion. The metallic surfaces of electrodes can also be ionized by the incident radiation, resulting in emission of electrons. The unipolar corona formed by the external applied voltage is a source of unipolar ions. Photoionization of molecules in the gas space leads to a bipolar atmosphere containing free positive and negative ions and electrons.

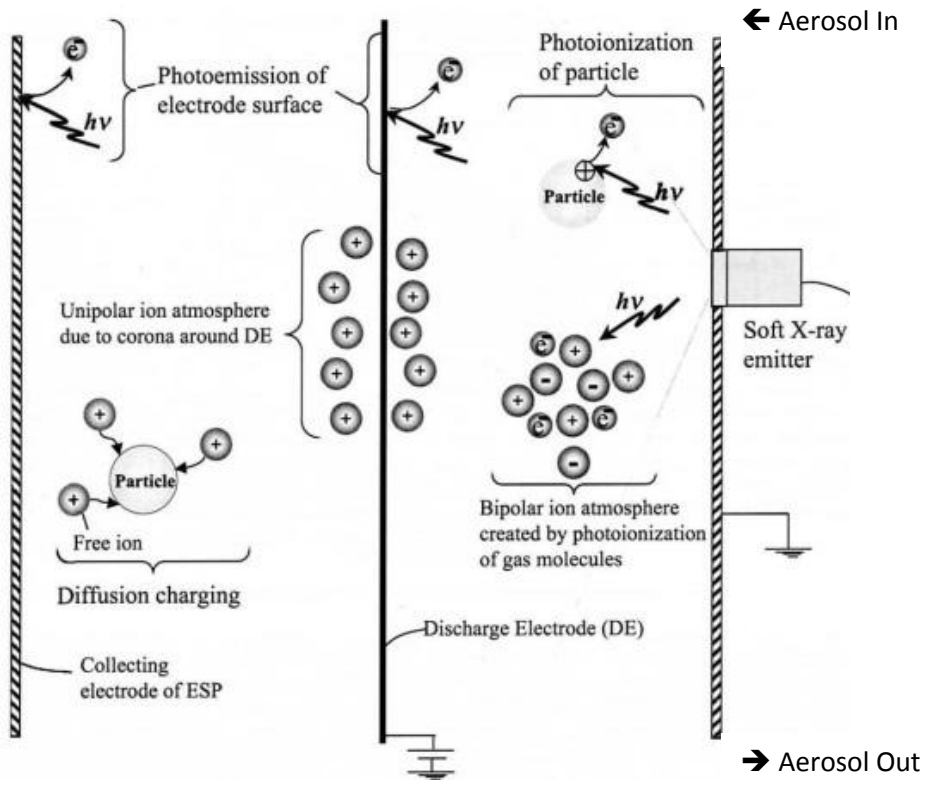


*Figure 2: Schematic diagram explaining the diffusion and direct particle charging and photoemission processes inside the ESP in the presence of corona and X-Ray radiation [2].*

The schematic diagram of the experimental setup is shown in Figure 3. The system consists of a particle generation system, an ESP, an aerosol size distribution measurement system (SMPS) and a particles counter (CPC). Aerosolized particles were first charge-neutralized using Kr-85 bipolar charger, were sort by size in a DMA column (Differential Mobility Analyzer), the particle

size distribution was control using a SMPS and the number of particles was counted using a CPC. Particles were then introduced in the ESP, exiting particles were also counted using a CPC. In the ESP, a DC voltage was applied across the collecting and discharge electrodes using a high voltage DC power supply. A DC micro ammeter was used to measure the voltage-current characteristics of the ESP.

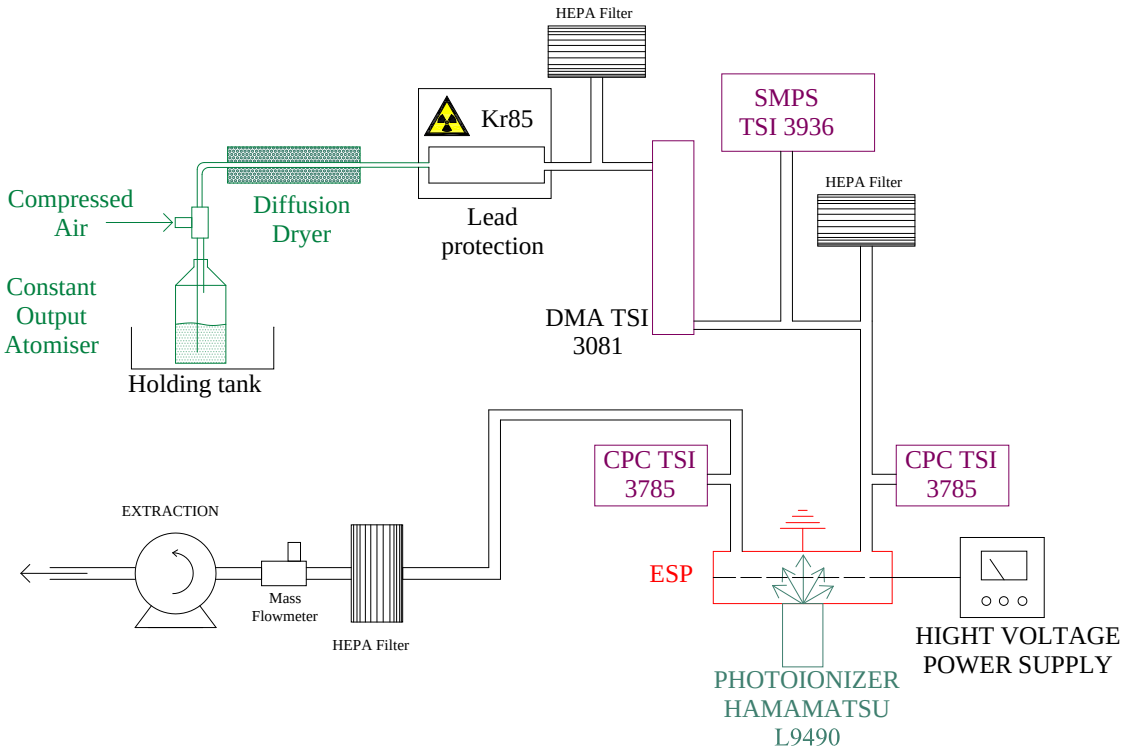


*Figure 3: Schematic diagram of the experimental setup used to measure particle capture efficiency of ESP with and without X-ray irradiation.*

The ESP consisted of a cylindrical, stainless steel collection electrode surrounding a discharge electrode. The collecting electrode was enclosed on the outside by a polyvinyl chloride (PVC) tube to shield against leaking X-rays. A circular hole was drilled in the middle of the PVC tube and collection electrode through which a fitted soft X-ray emitter (model L6941-1 from Hamamatsu Photonics Ltd., Japan) could irradiate the region inside the ESP. A high-voltage power supply was used to apply a potential difference between the centrally located charging electrode and the cylindrical collection electrode (Figure 4). The discharge electrode (DE) was made of stainless steel with a diameter of 0,5mm. The diameter of the tube was 5cm.
Before doing real experiments, we tested the sealing of the device against X-ray because the photoionizer irradiate in all the ESP and for the safety of user, X-ray emission must be below 0.1µSv/h at 10 cm of the device. Different configurations have been tested, see Figure 5. The first configuration investigated was those without tip (Figure 5 (a)). When the photoionizer was ON, we measured an X-ray emission of about 10mSv/h at the entry of the photoionizer noted *. We added a PolyEthylene (PE) tip to close the ESP and the X-ray emission decreased to about 2µSv/h (Figure 5 b). Putting one and two PolyVinylChloride (PVC) shutters in the PE tip (Figure 5 c, d, and g) decreased the X-ray emission to 0.5µSv/h and 0.1µSv/h respectively. When the both PE tips were replaced by 2 PVC tips, we observed that the X-ray emission still reduced. PVC was a better absorbing X-ray material compared to PE. The last configuration tested was those with curved tips at each sides of the device (Figure 5f). With this kind of

configuration, the X-ray emission was below 0.1µSv/h and it was the safer configuration and the used one for all the experiments made.

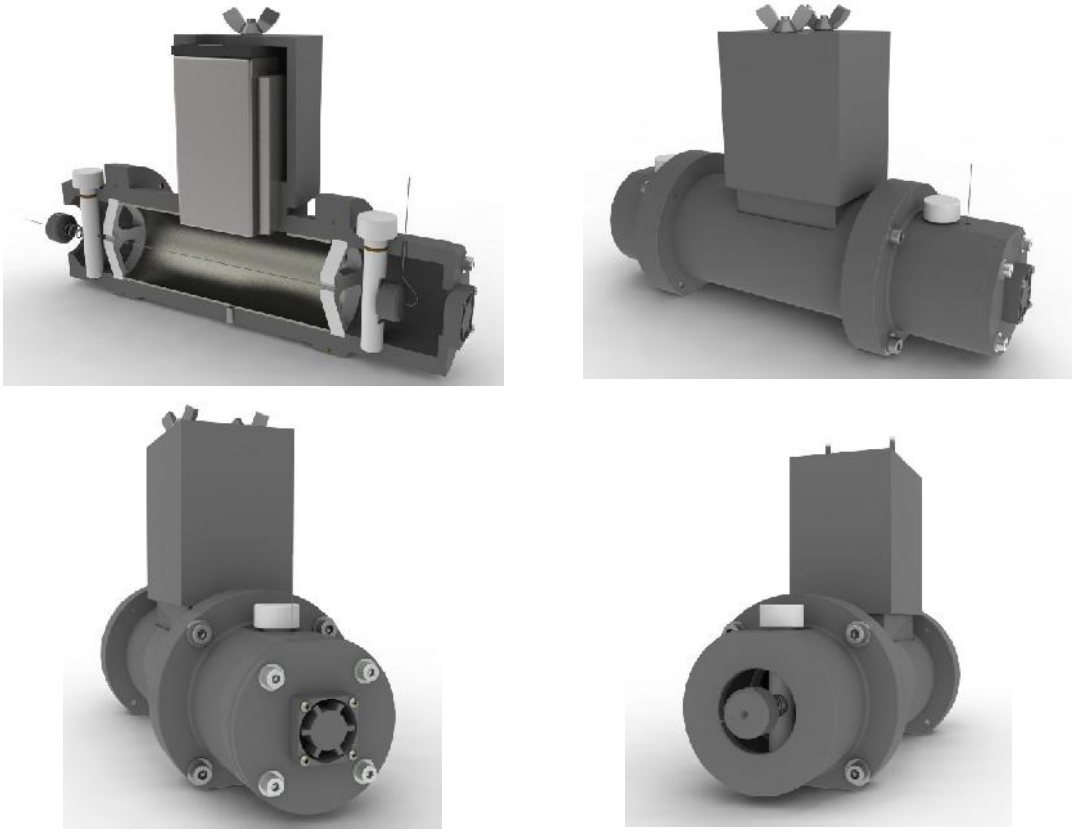

*Figure 4: Different drawings of the ESP with the photoioniser.*

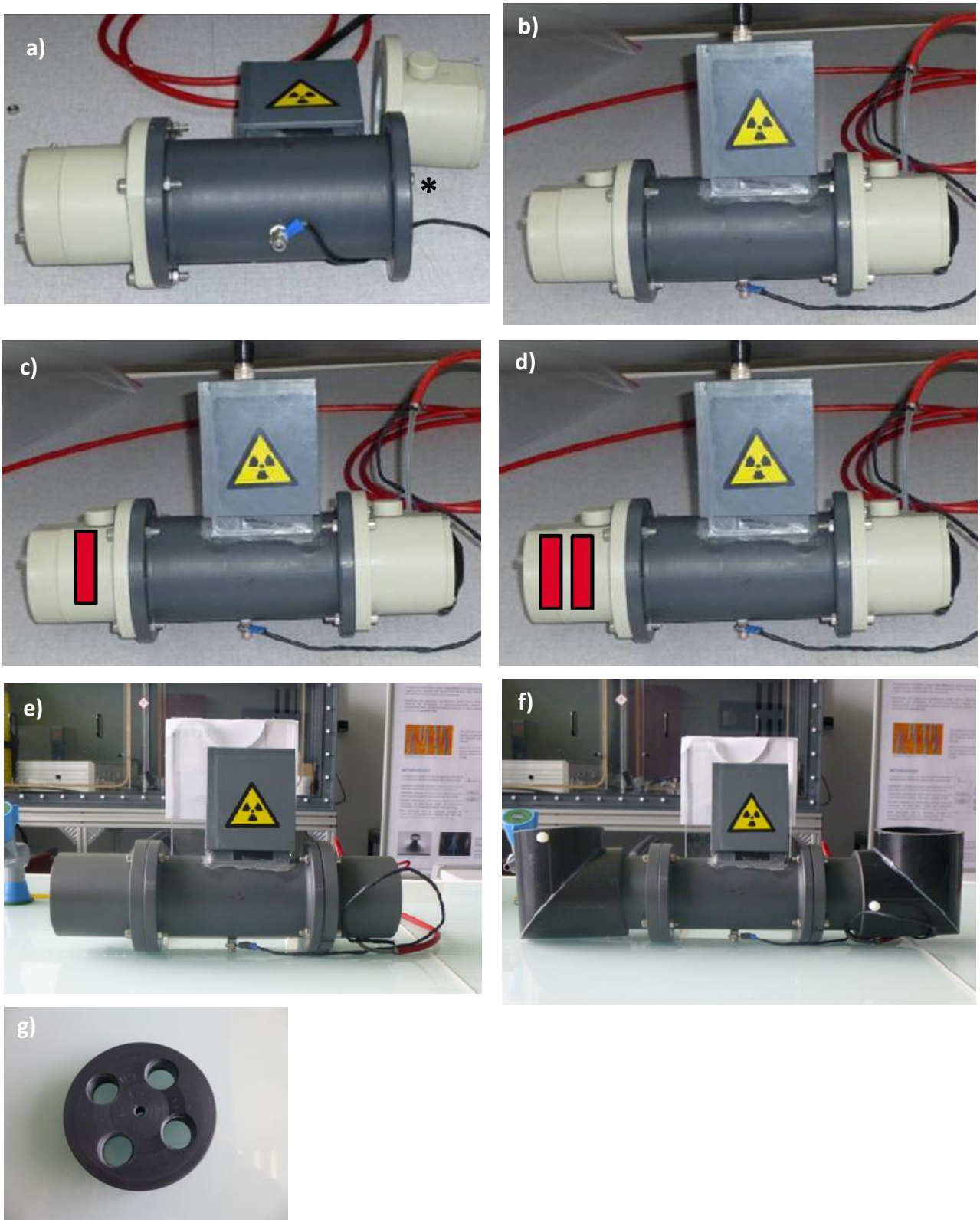


*Figure 5: Different pictures showing improvements of the set up done against the X-Ray emission outside.*

| Configuration | RX emission |
|---|---|
| Without tip | 10mSv/h |
| With PE tip | 2µSv/h |
| With PE tip and 1 PVC shutter | 0,5µSv/h |
| With PE tip and 2 PVC shutters | 0,1µSv/h |
| With PVC curved tip | <0,1µSv/h |

*Table 1: X-Ray emission measured outside the ESP set up.*

2) Experiments and results:

The first test performed was to determine the corona voltage of the ESP and to obtain the corona-current (I) characteristics over the entire range of operating voltages (V), with and without X-ray irradiation. A corona discharge is an electrical discharge brought on by the ionization of a fluid surrounding a conductor that is electrically energized. The discharge will occur when the strength (potential gradient) of the electric field around the conductor is high enough to form a conductive region, but not high enough to cause electrical breakdown or arcing to nearby objects. It is often seen as a bluish (or other color) glow in the air adjacent to pointed metal conductors carrying high voltages. Figure 6 shows the voltage-current characteristics of the ESP with X-ray irradiation.

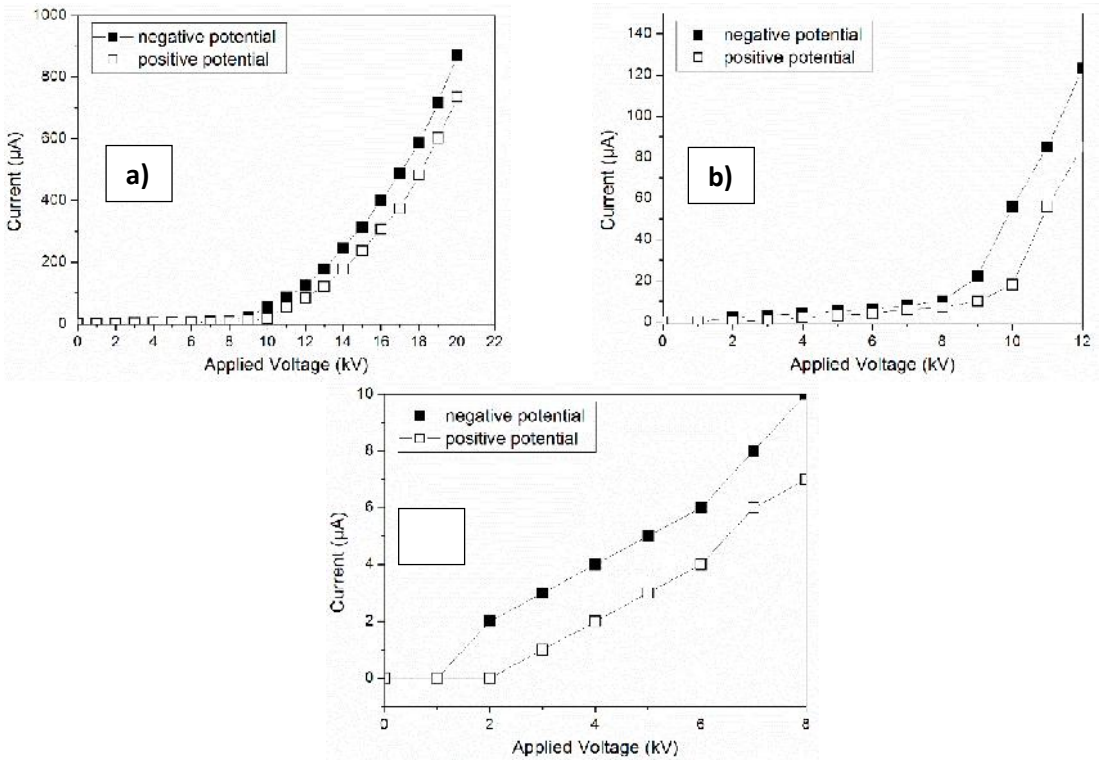


*Figure 6: Intensity/Voltage curves obtained at different voltage scales.*

On Figure 6 a), we saw the complete I/V curve. Until 8kV, the current through the ESP system was very low and at about 8kV, it increased rapidly and electric arcs appeared at 20kV. On Figure 6 b), we focused between 0 and 12kV in applied voltage. We clearly saw that the voltage increased significantly between 9-10kV, which could be the corona voltage. To be sure, we calculated the expected corona voltage and we obtained 10,2kV (see annex 1) which is in agreement with the observed value. Before this value, we observed on Figure 6 c) that the voltage was not equal to zero and that low voltages appeared at 2kV for negative potential and at 3kV for positive potential. In order to explore this low voltage effect, without corona effect, we investigated voltage ranges between +3 and +6kV for the positive voltage and between -2 and -6kV for the negative voltage.

The charging efficiency of the particle depends on various factors such as their physical characteristics (influences the direct photoionization as well as the diffusion charging efficiency), chemical composition (photoionization threshold could be different for each material; affects direct photoionization) and the number concentration of the aerosol in the gas space (affects the scattering of the X-ray radiation and hence direct photoionization, as well as photoemission from surface of the metal electrodes). That's why several parameters were investigated in this study as the influence of the voltage, of the photoionization effect, of the chemical nature of the NPs and of the NPs diameter on the collection efficiency.

Figures 7, 8 and 9 showed that the collection efficiency of all the investigated NPs followed the same behaviour. We observed that the capture efficiency increased with increasing the applied voltage. It was at zero when no voltage was applied and it increased between 30% for the worst cases to 100% for the best cases. Even if the corona voltage was not reached, we saw surprisingly an effect on the capture efficiency.

We observed also on these Figures (7, 8 and 9) that the implementation of a *in situ* soft X-ray irradiation generally enhanced the capture efficiency of $SiO_2$, $TiO_2$, nanoclay and nanocellulose particles for both positive and negative applied potential conditions. Capture efficiency was increased 1.5 time to 4 time depending on the magnitude of the applied voltage. More precisely, we observed that the capture efficiencies were better for negative applied voltages compared to the same positive magnitude.

In order to study the capture efficiency as a function of the NPs size, we selected 3 different sizes of NPs that composed the aerosols with a DMA column: 25nm, 50nm and 100nm. We can see on Figure 10, ESP collection alone (without the photoionizer, noted ESP afterwards) for the smallest NPs (25nm) was very efficient whatever the chemical composition of the NPs ($SiO_2$, $TiO_2$, nanoclay and nanocellulose). This was due to the highly efficient of charge diffusion of these very small particles. The efficiency of the photoionizer was only observed for the neutral ones which was not collected by the ESP, it was nevertheless less efficient for nanocellulose NPs (Figure 7 d)).
Results were different for the other NPs sizes. We saw for the 50nm and the 100nm sizes (Figure 8 and 9) that the ESP efficiency capture was lower than for the small ones and that the photoionizer helped the collection of those NPs for the neutral, the negative and the positive charged ones. The biggest particles have a bigger specific surface area and thus have more electrical charges at their surfaces. That's why they can be more easily deflected and captured by the PI as seen on Figures 10, 11 and 12. For the 50nm size, we observed that the capture efficiency did not reach 100% for all the voltages and that for the 100nm NPs, capture efficiency never reached 100% except for $TiO_2$ which seemed to be more captured by the X-ray irradiation (Figure 9), the chemical nature of the NPs influenced the efficiency of collect. By observing Figures 10 and 12, we saw that nanoclays were the most collected NPs whatever their sizes. Even NPs of 100nm in size were collected with a high efficiency.

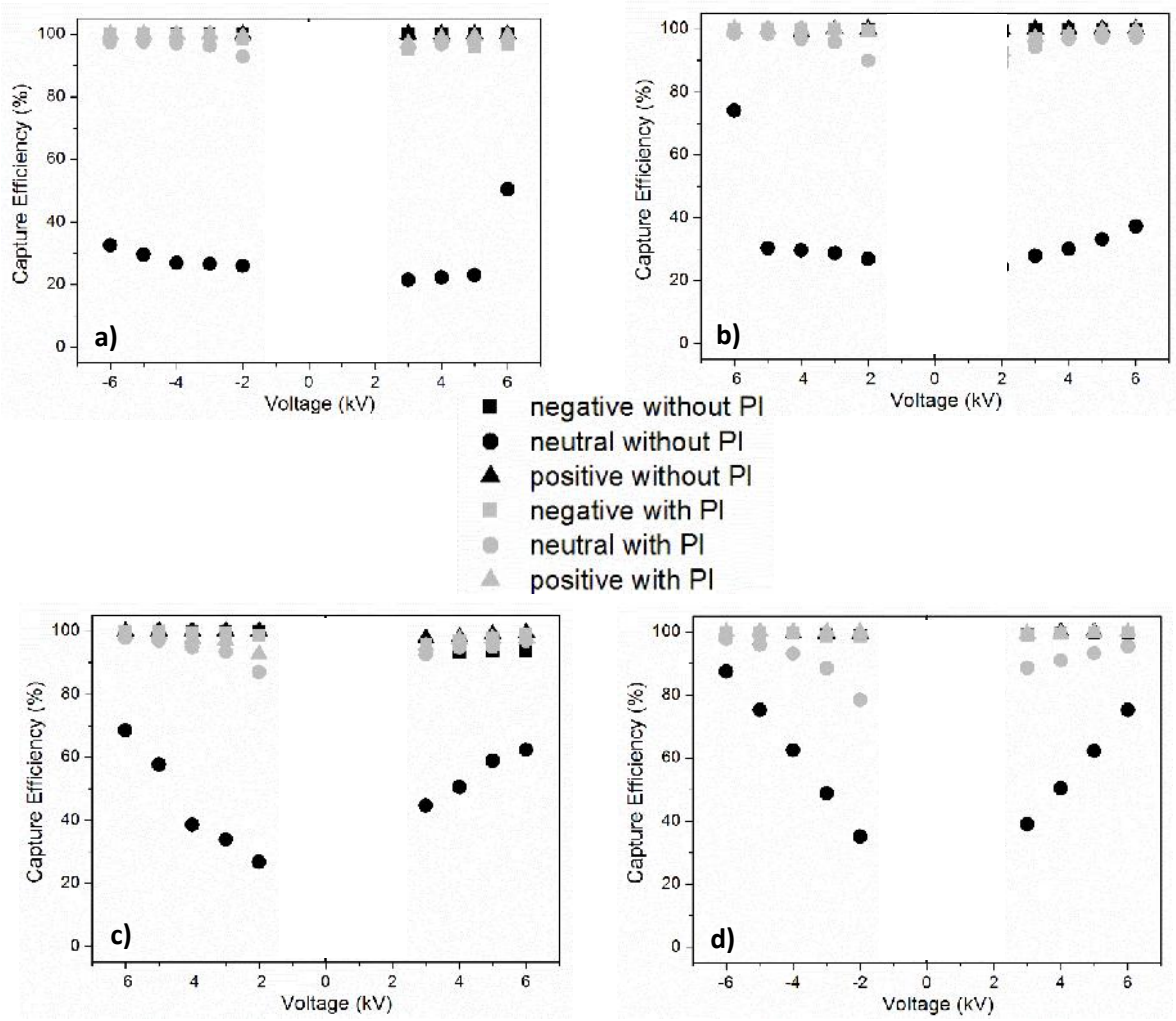


*Figure 7: Capture efficiency in function of voltage for a) $SiO_2$, b) $TiO_2$, c) nanoclay and d) nanocellulose NPs of 25nm of diameter with and without the action of the photoionizer.*

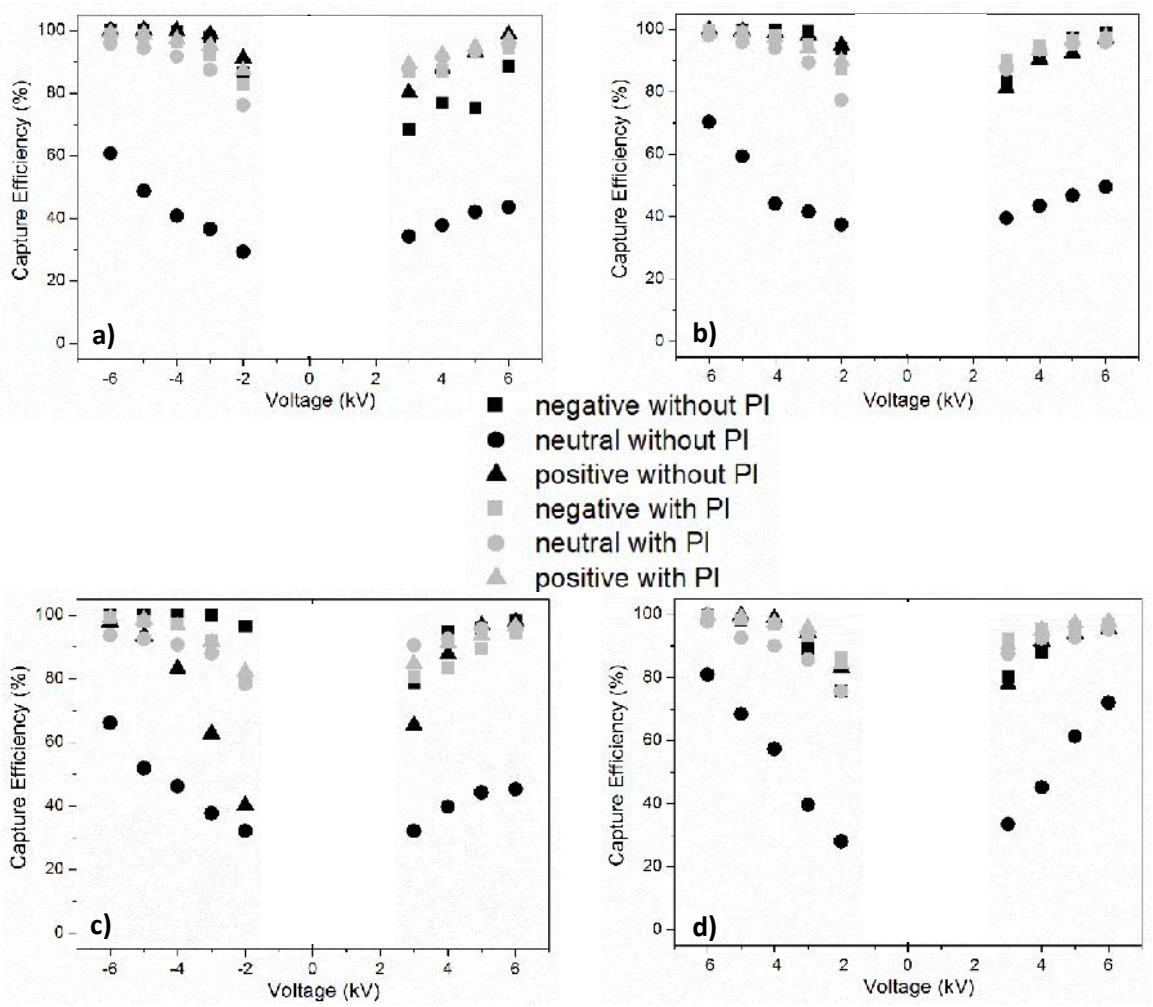


*Figure 8: Capture efficiency in function of voltage for a) $SiO_2$, b) $TiO_2$, c) nanoclay and d) nanocellulose NPs of 50nm of diameter with and without the action of the photoionizer.*

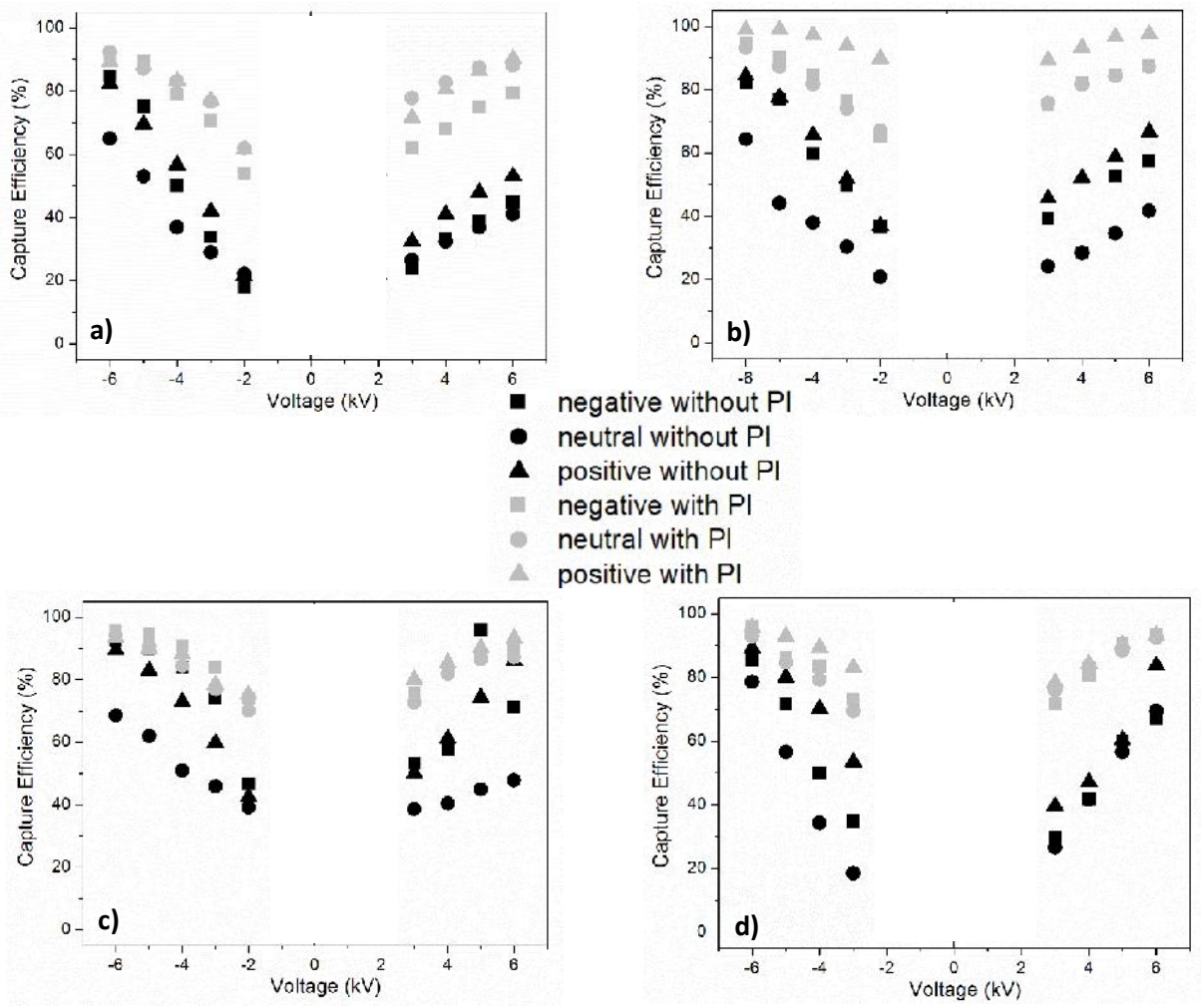


*Figure 9: Capture efficiency in function of voltage for a) $SiO_2$, b) $TiO_2$, c) nanoclay and d) nanocellulose NPs of 100nm of diameter with and without the action of the photoionizer.*

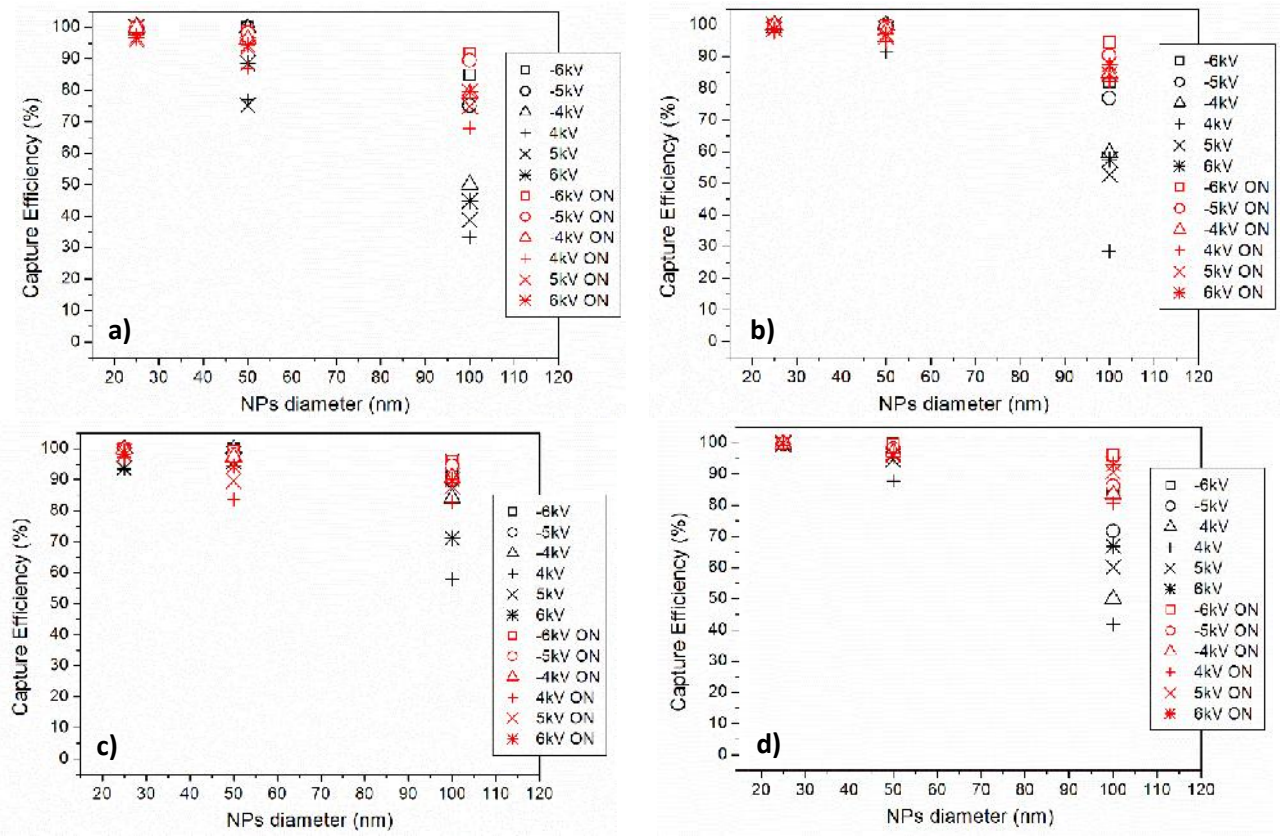


*Figure 10: Capture efficiency in function of the NPs diameter for negatively charged a) $SiO_2$, b) $TiO_2$, c) nanoclay and d) nanocellulose NPs with and without the action of the photoionizer.*

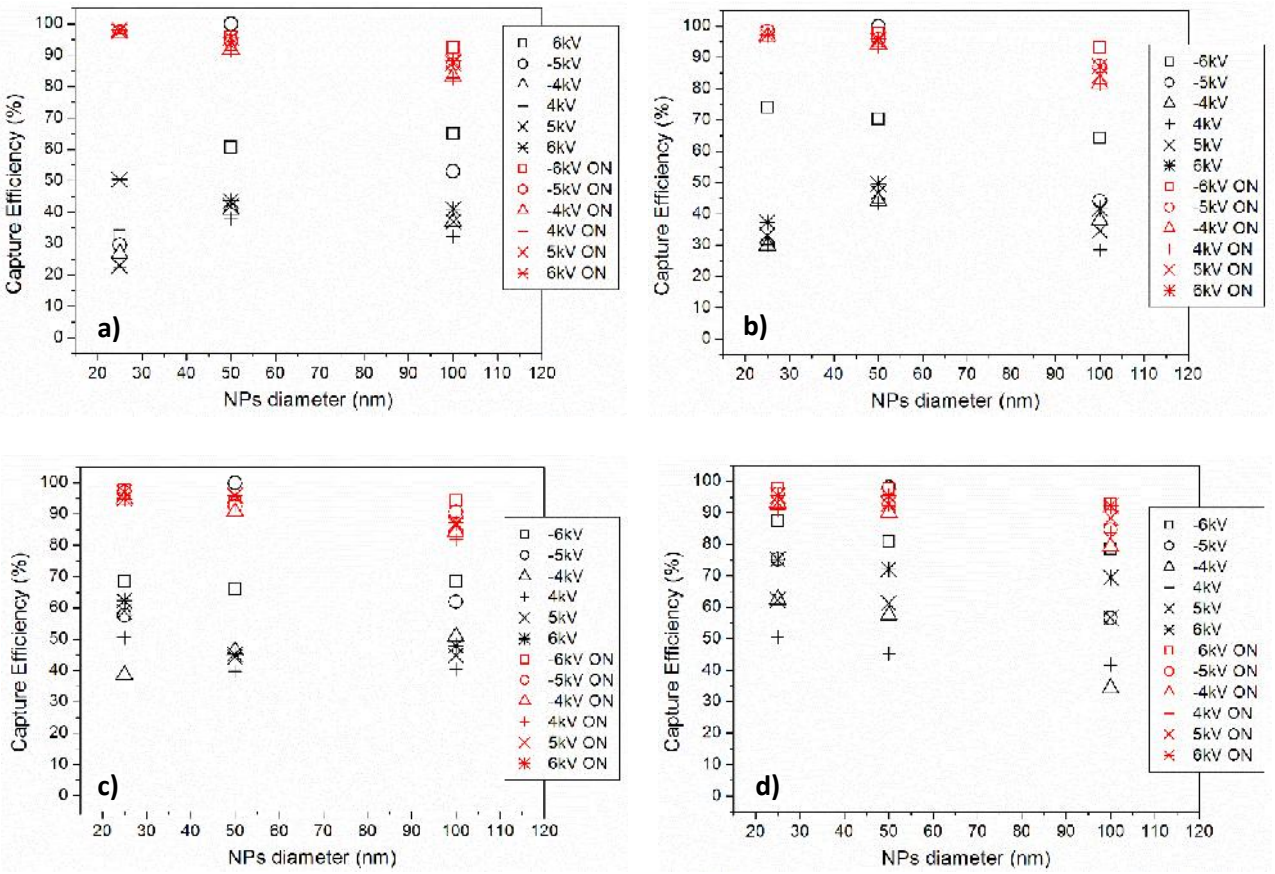


*Figure 11: Capture efficiency in function of the NPs diameter for neutral a) $SiO_2$, b) $TiO_2$, c) nanoclay and d) nanocellulose NPs with and without the action of the photoionizer.*

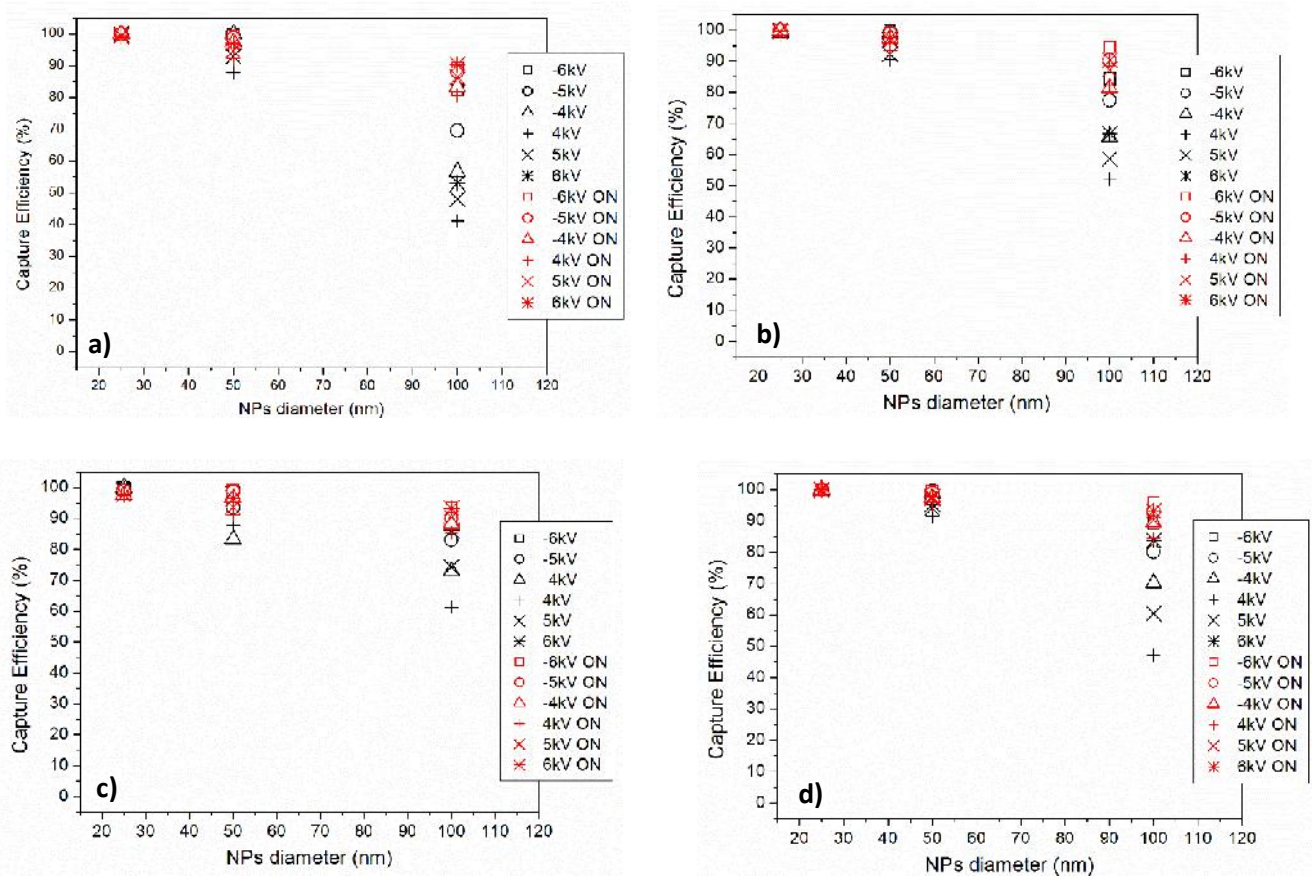


*Figure 12: Capture efficiency in function of the NPs diameter for positively charged a) $SiO_2$, b) $TiO_2$, c) nanoclay and d) nanocellulose NPs with and without the action of the photoionizer.*

# 4. CONCLUSIONS

The study revealed that we do not need the corona effect to collect efficiently ultrafine NPs [1, 2, 3]. As many workers studied the capture of NPs in the voltage range of the corona effect, we decided to investigate lower voltages. With the configuration studied, we calculated an Inception Corona Voltage of about 10kV. The investigated range was below this value, between 0 and ±6kV. We observed that even at very low voltage, ESP and ESP+PI were efficient. $SiO_2$, $TiO_2$, nanoclay and nanocellulose NPs of 25, 50 and 100nm of diameter were investigated. ESP alone was very efficient for the smallest NPs (25nm) negatively and positively charged, whatever the type of NPs. Addition of the PI effect enhanced the capture of the bigger NPs (50 and 100nm) for the negative, positive AND neutral charged NPs. Giving conclusions on the capture efficiency in function of the chemical nature of the NPs was quite difficult. ESP alone seemed to be more efficient for the collect of nanoclays and ESP+PI was more efficient for the capture of $TiO_2$ NPs. Our future work will be focused on the voltage range of the corona voltage to investigate the total voltage range until breakdown (electric arc).

## 5. FIGURES

## 6. TABLES



## 7. REFERENCES

1) Experimental and theoretical studies of ultra-fine particle behavior in electrostatic precipitators, Y. Zhuang *et al.* Journal of Electrostatics 48 (2000) 245-260
2) Charging of particles in unipolar coronas irradiated by *in situ* soft X-rays: enhancement of capture efficiency of ultrafine particles, P. Kulkarni *et al*., Aerosol Science 33 (2002) 1279-1296.
3) Soft X-Ray enhanced electrostatic precipitation for protection against inhalable allergens, ultrafine particles and microbial infections, E.M. Kettleson *et al.*, Applied and Environmental Microbiology, 79 (2013) 1333-1341

# 8. ANNEXES

**Corona Voltage calculation:**

1) Critical Field calculation:

Critical Field in kV/cm = $Ecc = Es\delta\left(1 + \frac{k}{\sqrt{\delta r}}\right)$

With Es = 30kV/cm (superficial electric field given by the Gauss theorem)

$\delta$ = air density = 1 in normal conditions

k = 0,308 (is a constant)

r = radius of the wire = 0,025cm

**Ecc = 88,4 kV/cm**

2) Inception Voltage calculation:

Inception Voltage in V = INCV = $r\ ln\left(\frac{dt}{dw}\right) * Ecc$

With r = radius of the wire = 0,025cm

dt = tube diameter = 5cm

dw = wire diameter = 0,05cm

**INCV = 10,2 V**